CHIN. PHYS. LETT. Vol. 29, No. 4 (2012) 046803

Mapping the Diffusion Potential of a Reconstructed Au(111) Surface at Nanometer Scale with 2D Molecular Gas *

YAN Shi-Chao(颜世超)[1], XIE Nan(谢楠)[1,2], GONG Hui-Qi(宫会期)[1], SUN Qian(孙骞)[2], GUO Yang(郭阳)[1], SHAN Xin-Yan(单欣岩)[1], LU Xing-Hua(陆兴华)[1]**

[1]*Beijing National Laboratory for Condensed-Matter Physics and Institute of Physics, Chinese Academy of Sciences, Beijing 100190*

[2]*Photonics Center, College of Physics Science, Nankai University, Tianjin 300071*

(Received 26 February 2012 and accepted by WANG Ding-Sheng)

The adsorption and diffusion behaviors of benzene molecules on an Au(111) surface are investigated by low-temperature scanning tunneling microscopy. A herringbone surface reconstruction of the Au(111) surface is imaged with atomic resolution, and significantly different behaviors are observed for benzene molecules adsorbed on step edges and terraces. The electric field induced modification in the molecular diffusion potential is revealed with a 2D molecular gas model, and a new method is developed to map the diffusion potential over the reconstructed Au(111) surface at the nanometer scale.

PACS: 68.35.bd, 68.43.Jk, 68.43.Fg DOI: 10.1088/0256-307X/29/4/046803

Surface diffusion of adsorbates plays an important role for surface mediated chemical reactions, especially for surface catalysis in which the molecules diffuse to the "hot spot" for the reactions to occur.[1−3] Gold is an effective catalyst for chemical reactions such as CO oxidation and NO reduction, and great efforts have been made out to understand its fundamental properties at the nanometer and atomic scales.[4,5] Scanning tunneling microscopy (STM) studies have revealed the adsorption and diffusion behaviors of various molecules on gold single crystal surfaces,[2,3,6−11] particularly on the Au(111) surface which possesses a complex $22\times\sqrt{3}$ herringbone reconstruction.[12,13] The reconstructed Au(111) surface exhibits a gradually varied diffusion potential landscape with discrete strong bonding sites that serve as anchors for molecular self-assembly.[8,9] Measuring the diffusion potential over the whole $22\times\sqrt{3}$ unit cell, however, still remains a challenge. This is because the traditional STM methods in studying surface diffusion, i.e. real-time molecular tracking[14−16] and "image-anneal-image" mode,[17] cannot be applied to the gradually varied potential surfaces.

In this Letter, we report a new STM method to map the diffusion potential of a herringbone reconstructed Au(111) surface at nanometer scale with adsorbed benzene molecules. At coverage below the 0.9 monolayer, benzene molecules are mobile on the Au(111) terraces even at low temperatures of 10 K, forming a two-dimensional molecular gas.[2] Such molecular gas occupies the surface area of low potential energy, and the pattern can be imaged. Further, with the aid of the scanning tip, we are able to gradually tune the diffusion potential directly beneath the tip and thus the diffusion potential for the whole surface can be mapped.

Our experiments were conducted using a home-built ultrahigh-vacuum (UHV) STM operated at 10 K.[18] The Au(111) single crystal substrate was cleaned by cycles of Ar^+ ion sputtering and annealing at 900 K. Benzene was purified by several freeze-pump-thaw cycles and then introduced into the chamber via a variable-leak valve after the sample was cooled to 10 K. Chemically etched Ag wire was used as the STM tip in this study. The bias voltages here refer to the sample bias with respect to the tip.

Figure 1(a) shows a typical STM image of the clean Au(111) surface before molecular deposition. Both the surface reconstruction and the surface standing waves are clearly resolved. The standing waves, induced by the scattering of the surface electronic state at the steps, are parallel to the edges. The $22\times\sqrt{3}$ herringbone reconstruction is exhibited as pairs of corrugation lines. The periodicity of the paired lines is about 63 Å and the vertical corrugation amplitude is about 0.3 Å. The wider and narrower depressions between corrugation lines are associated with fcc and hcp stacking regions, respectively.[12] Figure 1(b) shows the herringbone reconstruction on large flat terraces, with the inset showing an atomic-resolved Au(111) surface image. The ±120° bending of the corrugation lines results from the rotational domains of the $(22\times\sqrt{3})$ structure.[12]

At low coverage, benzene molecules prefer to adsorb on the step edges of metal surfaces, as shown in Fig. 2(a). The most preferred adsorption site is along

*Supported by the National Basic Research Program of China under Grant No 2012CB933002, and the National Natural Science Foundation of China under Grant No 11174347.

**Correspondence author, Email: xhlu@iphy.ac.cn

the step edge of the fcc-stacked region. As a consequence, one-dimensional benzene chain segments are formed along the edges in the fcc region, while the hcp region remains almost unoccupied. The average distance between molecules is about 8.2 ± 0.1 Å. Due to the Smoluchowski effect,[19] the electron flows from the upper to the lower terrace and results in a relatively higher unfilled local density of states (LDOS) at the upper terrace than that at the lower terrace. Being nucleophilic on the Au(111) surface, benzene is an electron donor and therefore prefers to bind at the upper step edges.[2] By increasing molecular coverage, the step edges of the fcc region are mostly filled up before additional benzene molecules start to fill the hcp region, as indicated by the red circle in Fig. 2(a). A similar adsorption site selectivity on the stepped Au(111) surface has been reported for other larger molecules, such as nitronaphtalene and fullerene.[20,21] According to recent DFT calculations, the adsorption energy of benzene along the step edge in the fcc region is 80 meV, more stable than that in the hcp region,[22] which is consistent with our experimental observations.

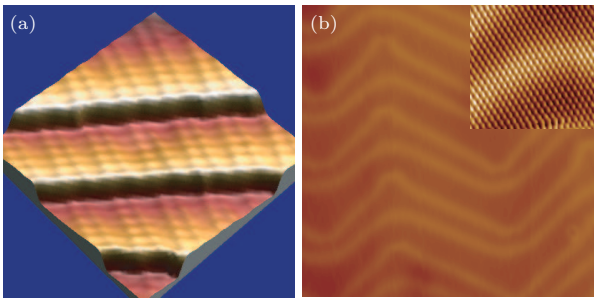

Fig. 1. STM constant current images of the reconstructed Au(111) surface at 10 K. (a) STM image of the stepped Au(111) surface (36 nm × 36 nm, $V_{\text{sample}} = -0.1$ V, $I_t = 0.1$ nA), (b) STM image of the Au(111) terrace (36 nm × 36 nm, $V_{\text{sample}} = -0.5$ V, $I_t = 0.26$ nA). The inset shows the atomic resolved herringbone structure.

On the terraces, benzene molecules are mobile and can only be stably imaged in the herringbone elbow regions or around the point defects, as shown in Fig. 2(b). At about 0.5 monolayer coverage, the mobile molecules can be imaged when the sample bias is increased from −2.0 V to −1.0 V, and appear as a uniform bright pattern in the STM image (Figs. 2(c) and 2(d)). This pattern results from the diffusion of the benzene molecules under the STM tip,[7] and varies as the sample bias changes. Figures 3(a)–3(d) show a sequence of STM images on a flat Au(111) terrace acquired with different sample biases. At −2.5 V, no mobile benzene molecules can be observed, besides the stationary molecules in the elbow regions, as shown in Fig. 3(a). The uniform bright pattern gradually shows up as the sample bias increases from −1.8 V to −0.5 V (Figs. 3(b)–3(d)). For sample bias at or above −0.5 V, the pattern fills up the whole surface except the corrugation lines of the herringbone reconstruction.

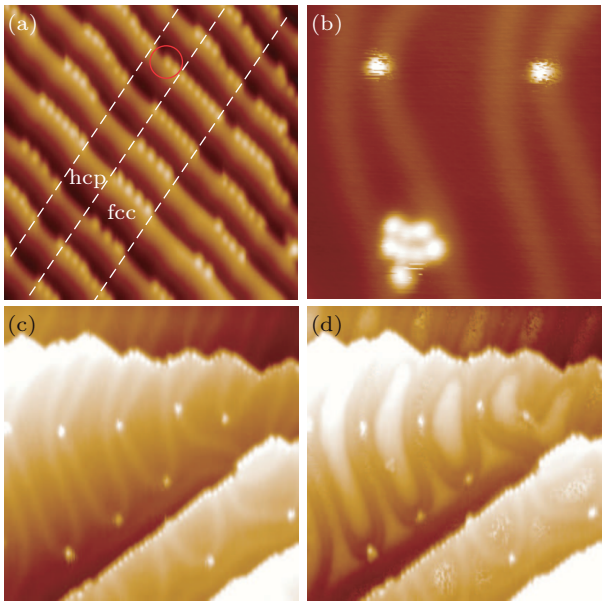

Fig. 2. Adsorption and diffusion of benzene molecules on an Au(111) surface. (a) STM image of molecules on Au(111) step edges (24 nm × 24 nm, $V_{\text{sample}} = -1.0$ V, $I_t = 0.1$ nA). The dashed lines and the red circle indicate corrugation lines and the molecule in the hcp region, respectively. (b) STM image of molecules around surface defect points and herringbone elbow sites (12 nm × 12 nm, $V_{\text{sample}} = -2.0$ V, $I_t = 0.1$ nA). The STM images of the molecules on the reconstructed Au(111) terrace with image size 36 nm × 36 nm: (c) for $V_{\text{sample}} = -2.0$ V and $I_t = 0.1$ nA, (d) for $V_{\text{sample}} = -1.0$ V and $I_t = 0.1$ nA.

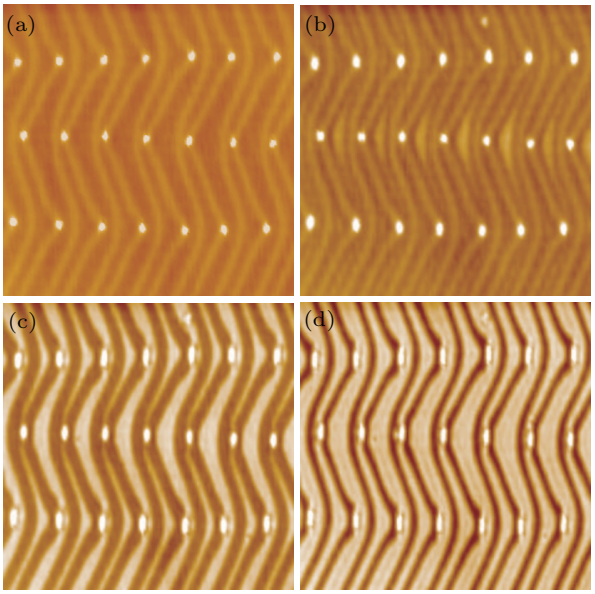

Fig. 3. A sequence of constant current STM images taken at (a) −2.5 V, (b) −1.8 V, (c) −1.0 V and (d) −0.5 V sample biases. The current is 10 pA, and the scan size is 45 nm × 45 nm.

In order to interpret the evolution of the pattern for mobile molecules, we consider the effect of the local electric field induced by the STM tip. Due to the high work function of the Au surface and the nucleophilicity

of the benzene molecule, there is charge transfer from benzene to the substrate upon molecular adsorption, resulting in a local dipole moment $\boldsymbol{p}$ pointing from the substrate to the molecule. The dipole interacts with the local electric field $\boldsymbol{E}$ induced by an STM tip directly positioned on top of the molecule. The effective surface diffusion potential $U_0(\boldsymbol{r})$ is thus locally modified as follows:

$$U(\boldsymbol{r}, V) = U_0(\boldsymbol{r}) - \boldsymbol{p} \cdot \boldsymbol{E} = U_0(\boldsymbol{r}) - \alpha V, \qquad (1)$$

where V refers to the sample bias and α is a constant.

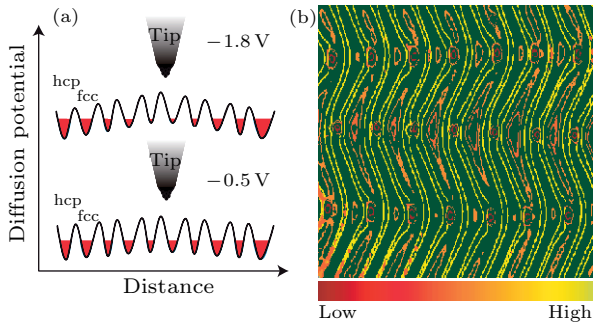

Fig. 4. (a) A schematic model for electric field modified diffusion potential. (b) Diffusion potential map of an Au(111) surface created from a series of STM images taken with sample biases from −2.0 V to −0.1 V.

Statistically, the molecules will fill into the area where the diffusion potential is lower than a critical energy U_C. The critical energy U_C represents the chemical potential of the 2D molecular gas, and its value depends on the molecular coverage. For a specific bias voltage V, the imaged molecular pattern is thus defined by $U(\boldsymbol{r}, V) < U_C$. As the sample bias increases from −2.0 V to −0.5 V, the local diffusion potential $U(\boldsymbol{r}, V)$ is lowered gradually, which results in the expansion of molecular patterns (as shown schematically in Fig. 4(a)). The boundary of the imaged molecular pattern is thus defined by $U(\boldsymbol{r}, V) = U_0(\boldsymbol{r}) - \alpha V = U_C$, which is just the equal-potential line for $U_0(\boldsymbol{r}) = U_C + \alpha V$. Thus, the contour map of diffusion potential $U_0(\boldsymbol{r})$ can be obtained by adding molecular pattern boundaries taken with various sample biases, as shown in Fig. 4(b).

By examining the obtained diffusion potential map shown in Fig. 4(b), several features are revealed at nanometer scale. First, the elbow site has the lowest diffusion potential, where molecules can be steadily adsorbed. Such a periodic elbow pattern has been a good template for self-assembled molecular arrays.[9] Second, the fcc region has a lower diffusion potential than the hcp region. Third, in both the fcc and hcp regions, the wide area has a relatively lower diffusion potential than the narrow area. Lastly, the corrugation lines have the highest diffusion potential, and no molecules are imaged on the lines even with a bias voltage of 3.0 V at 0.5 monolayer coverage.

In summary, we have developed a new method of mapping the diffusion potential of the Au(111) surface by employing electric field induced potential modification in 2D molecular gas. It is revealed that herringbone surface reconstruction plays an important role in determining the diffusion potential of the Au(111) terrace, as well as the step edges. The derived potential map provides a comprehensive scenario of the molecular diffusion dynamics on the Au(111) surface, which is beneficial to the understanding of the related surface chemical reactions and the design of electronic nanodevices.[7,23]

References

[1] Roberts M W 2000 *Catal. Lett.* **67** 41
[2] Han P, Mantooth B A, Sykes E C H, Donhauser Z J and Weiss P S 2004 *J. Am. Chem. Soc.* **126** 10787
[3] Sykes E C H, Mantooth B A, Han P, Donhauser Z J and Weiss P S 2005 *J. Am. Chem. Soc.* **127** 7255
[4] Carabineiro S A C and Nieuwenhuys B E 2009 *Gold Bull.* **42** 288
[5] Meyer R, Lemire C, Shaikhutdinov S K and Freund H 2004 *Gold Bull.* **37** 72
[6] Sykes E C H, Han P and Weiss P S 2003 *J. Phys. Chem.* B **107** 5016
[7] Jiang N, Zhang Y Y, Liu Q, Cheng Z H, Deng Z T, Du S X, Gao H J, Beck M J and Pantelides S T 2010 *Nano Lett.* **10** 1184
[8] Clair S, Pons S, Brune H, Kern K and Barth J V 2005 *Angew. Chem. Int. Ed.* **44** 7294
[9] Gao L, Liu Q, Zhang Y Y, Jiang N, Zhang H G, Cheng Z H, Qiu W F, Du S X, Liu Y Q, Hofer W A and Gao H J 2008 *Phys. Rev. Lett.* **101** 197209
[10] Zhao A D, Li Q X, Chen L, Xiang H J, Wang W H, Pan S, Wang B, Xiao X D, Yang J L, Hou J G and Zhu Q S 2005 *Science* **309** 1542
[11] Kuhnle A, Molina L M, Linderoth T R, Hammer B and Besenbacher F 2004 *Phys. Rev. Lett.* **93** 086101
[12] Barth J V, Brune H, Ertl G and Behm R J 1990 *Phys. Rev.* B **42** 9307
[13] Bulou H and Goyhenex C 2002 *Phys. Rev.* B **65** 045407
[14] Swartzentruber B S 1996 *Phys. Rev. Lett.* **76** 459
[15] Lauhon L J and Ho W 1999 *J. Chem. Phys.* **111** 5633
[16] Mitsui T, Rose M K, Fomin E, Ogletree D F and Salmeron M 2002 *Science* **297** 1850
[17] Mo Y W 1993 *Phys. Rev. Lett.* **71** 2923
[18] Stipe B C, Rezaei M A and Ho W 1999 *Rev. Sci. Instrum.* **70** 137
[19] Smoluchowski R 1941 *Phys. Rev.* **60** 661
[20] Vladimirova M, Stengel M, De Vita A, Baldereschi A, Bohringer M, Morgenstern K, Berndt R and Schneider W D 2001 *Europhys. Lett.* **56** 254
[21] Xiao W, Ruffieux P, Ait Mansour K, Groening O, Palotas K, Hofer W A, Groening P and Fasel R 2006 *J. Phys. Chem.* B **110** 21394
[22] Gaspari R, Pignedoli C A, Fasel R, Treier M and Passerone D 2010 *Phys. Rev.* B **82** 041408
[23] Suo Z and Hong W 2004 *Proc. Natl. Acad. Sci.* **101** 7874